九州大学学術情報リポジトリ
Kyushu University Institutional Repository

Relationship between impaired cardiac sympathetic activity and spatial dyssynchrony in patients with non-ischemic heart failure: Assessment by MIBG scintigraphy and tagged MRI

米澤, 政人

https://doi.org/10.15017/1441109

出版情報：九州大学, 2013, 博士（医学）, 課程博士
バージョン：
権利関係：やむを得ない事由により本文ファイル非公開（2）

KYUSHU UNIVERSITY

Relationship between Impaired Cardiac Sympathetic Activity and Spatial Dyssynchrony in Patients with Non-ischemic Heart Failure: Assessment by MIBG Scintigraphy and Tagged MRI

Journal of Nuclear Cardiology. 2013 Aug;20(4):600-8

Masato Yonezawa*, Michinobu Nagao†, Koichiro Abe*, Yoshio Matsuo*, Shingo Baba*, Takeshi Kamitani*, Takuro Isoda*, Yasuhiro Maruoka*, Mikako Jinnouchi*, Yuzo Yamasaki*, Kohtaro Abe‡, Taiki Higo‡, Takashi Yoshiura*, Hiroshi Honda*

*Department of Clinical Radiology,

†Molecular Imaging & Diagnosis, and ‡Cardiology

Graduate School of Medical Sciences, Kyushu University, Fukuoka, Japan

A concise and informative title: Cardiac Sympathetic Activity and Dyssynchrony in HF

ABSTRACT

Background. Impairment of cardiac sympathetic activity has various detrimental effects on cardiac function. The purpose was to investigate the relationship between left ventricular (LV) dyssynchrony and cardiac sympathetic activity in non-ischemic heart failure (HF).

Methods. Twenty-seven patients with non-ischemic HF were enrolled. Cardiac sympathetic activity was assessed by heart-to-mediastinum ratio (H/M ratio) on ^{123}I-Metaiodobenzylguanidine scintigraphy. LV dyssynchrony was assessed by cross-correlation analysis of time curves of myocardial circumferential strains delivered from cine-tagging MR images. Temporal dyssynchrony was defined as contraction delay between septal and lateral segments>110 milliseconds. Spatial dyssynchrony was defined as the negative value of the maximum correlation for the two strain time curves.

Results. H/M ratio was significantly lower for patients with spatial dyssynchrony compared to patients without (1.8 ± 0.3 vs 2.1 ± 0.3, $P < .05$). There was no difference between patients with and without temporal dyssynchrony (2.0 ± 0.2 vs 2.0 ± 0.3). The incidence of spatial dyssynchrony was significantly higher in patients with H/M ratio

<2.0 than those whose ratios were ‡2.0 (75% vs 20%, P 5 .001). There was no difference in the incidence of temporal dyssynchrony between the two groups (17% vs 20%).

Conclusion. Impairment of cardiac sympathetic activity was found to be associated with spatial dyssynchrony in patients with non-ischemic HF.

Key Words: Heart failure Æ sympathetic activity Æ dyssynchrony Æ MIBG Æ tagging MRI

INTRODUCTION

Patients with heart failure (HF) show increased activation of the sympathetic nervous system, as reflected by an increase in plasma norepinephrine levels. It is well known that the neuronal uptake of norepinephrine is impaired in the failing myocardium. The enhanced release of norepinephrine and changes in its cardiac neuronal uptake may be responsible for the observed downregulation of adrenoreceptors in patients with HF.(1) ^{123}I-Metaiodobenzylguanidine (MIBG), a presynaptic imaging agent, is a norepinephrine analog^{123}I-Metaiodobenzylguanidine (MIBG), a presynaptic imaging agent, is a norepinephrine analog which is concentrated and stored in the myocardium in a fashion similar to the norepinephrine.(2) MIBG imaging has been widely used for the assessment of cardiac sympathetic function in HF.(3-5) Several research groups found that impaired cardiac adrenergic innervation as assessed by MIBG imaging was closely associated with mortality in patients with HF.(6-8)

Left ventricular (LV) dyssynchrony with QRS prolongation, thought to denote intraventricular conduction abnormalities, is present in more than 25% of patients with HF and has been associated with a poor prognosis.(9) Although LV dyssynchrony has a

detrimental effect on LV systolic and diastolic functions in HF patients, the effect of LV dyssynchrony on cardiac sympathetic activity is not yet fully understood.

Accordingly, our objective in this study was to evaluate by means of MIBG scintigraphy the effect of LV dyssynchrony on the cardiac sympathetic activity of HF patients with non-ischemic HF.

Methods

Patient population

The study protocol was reviewed and approved by the institutional review board, and written informed consent was obtained from all patients.

Thirty-six consecutive patients with HF, who had recent NYHA classes II, III, or IV symptoms and had been admitted to our hospital between June 2010 and April 2012 were prospectively enrolled in this study. In all patients, cardiac MRI, MIBG scintigraphy, transthoracic echocardiography, electrocardiogram, and blood testing for brain natriuretic peptide (BNP) were performed to diagnosis or determine the treatment strategy within 2 weeks before or after the cardiac MRI. Exclusion criteria were:

patients who had a history of myocardial infarction and/or a coronary angiogram indicating major disease and/or a history of coronary artery bypass graft and/or angioplasty, unstable angina, previously implanted pacemaker or cardioverter-defibrillator, other implanted devices or metal objects contraindicated for a magnetic resonance scanner, renal failure with glomerular filtration rate (GFR) levels<50 mL/kg/1.73 cm2, claustrophobia, significant arrhythmia including atrial fibrillation, limited mobility, life expectancy due to other co-morbidities<1 year, history of heart transplant, pregnancy, and lack of informed consent to participate in the study.

Patients were defined as having dilated cardiomyopathy (DCM) or hypertrophic cardiomyopathy (HCM) based on the guidelines for diagnosis.(10-12) Patients were defined as having hypertensive heart disease (HT) if they had had essential hypertension for many years and did not satisfy the principal diagnosis of DCM, HCM, or ischemic heart disease (IHD).(13,14) Nine patients with pulmonary hypertension (15), who had normal LV function were enrolled as controls for patients to determine a normal range of MIBG uptake or LV dyssynchrony with tagged MRI.

In 4 of the 36 patients (DCM: 3, HCM: 1), cardiac resynchronization therapy

(CRT) was performed within 3 months after the cardiac MRI. In two of the 36 patients, a left ventricular assist device (LVAD) was implanted for cardiac transformation. Table 1 indicates all patients' characteristics.

Cardiac MR imaging

All patients underwent 3.0T MR imaging (Achieva 3.0T Quarsar Dual; Philips Healthcare, Best, The Netherlands) equipped with dual-source parallel radiofrequency (RF) transmission, 32-element cardiac phased-array coils used for RF reception, and a four-lead vector cardiogram used for cardiac gating. Cine balanced turbo field-echo sequences in two-, three-, and four-chamber views and a stack of short-axis images acquired in parallel to the atrioventricular groove from the base to apex were performed with the following imaging parameters: repetition time 3.3 milliseconds, echo time 1.4 milliseconds, flip angle 45°, slice thickness 10 mm, field of view 380 mm, matrix size 256 × 160, SENSE factor 2, 20 cardiac phases/R-R interval on ECG.

Tagged cine images in basal, mid, and apical short-axis views were acquired

using an ECG-triggered 2D turbo fieldecho sequence with a resting grid pulse, always before gadolinium injection (repetition time 4.6 milliseconds, echo time 2.7 milliseconds, flip angle 12°, section thickness 10 mm, field of view 380 mm, matrix size 256 × 179, SENSE factor 2, tag grid 5 mm, 20 cardiac phases/R-R interval on ECG). The basal slice was chosen so that it would not visualize the LV outflow tract or papillary muscles (Figure 1).

Image analysis

Cine images were analyzed with the use of dedicated software (Extended WorkSpace, Philips Healthcare, Best, the Netherlands). Initially, the short-axis images were previewed from the base to the apex in a cinematic mode, and then the endocardial and epicardial contours for end-diastole and endsystole were automatically extracted and partly manually traced. Delineated contours were used for the quantification of LV volumes and the LV ejection fraction (LVEF).

The assessment of dyssynchrony was based on myocardial strain time curves derived from 2D tagging imaging. The tagging imaging was analyzed using the

open-source software OsiriX (plugin: inTag toolbox) based on the Sine-wave modeling approach.(16) First, the phase of maximal systole and the area of interest were chosen. Subsequently, endocardial and epicardial contours were delineated semi-automatically. Circumferential strains were measured in septal and lateral segments at the basal, mid-, and apex of the LV wall.

Based on the cross-correlation analysis of the strain time curve,(17) the temporal delay was computed between the septal and lateral time curves by shifting one curve in time relative to the other curve and computing the normalized correlation between the curves for each time shift. The time shift between the two curves that resulted in the maximum correlation value was defined as the temporal delay between the two strain time curves (Figure 1). The temporal dyssynchrony time was defined as a septa-lateral cross-correlation delay averaged among the basal, mid-, and apical wall. Temporal dyssynchrony was defined as temporal dyssynchrony time>110 milliseconds. Spatial dyssynchrony was defined as the negative value of the maximum correlation of the two time curves at the mid-LV wall. The negative value of the maximum correlation means

that the peaks of the two strain time curves are opposite, suggesting dyskinetic wall motion in one of septal and lateral segment (Figure 2).

MIBG scintigraphy

Data acquisition and H/M ratio

Patients were injected intravenously with ^{123}I-MIBG (111 MBq) while in an upright position. Single-photon emission computed tomographic (SPECT) images were acquired 15 minutes after injection and repeated 4 hours later. Anterior and lateral planar images were acquired immediately after each SPECT acquisition. SPECT imaging was performed with a dual-head rotating gamma camera (Infinia Hawkeye, GE Medical Systems, Waukesha, WI) equipped with a low-energy, generalpurpose collimator. Images were acquired for 35 seconds each at 60 steps over a 360———————————— orbit and were recorded at a digital resolution of 64 9 64 pixels. A 20% energy window centered on 159 keV was used. The heart/mediastinum count (H/M) ratio was determined from anterior planar early and delayed 123I-MIBG images, where H is the mean count/pixel in the LV, and M is the

mean count/pixel in the upper mediastinum (Figure 1). The delayed H/M ratio was used as an estimate of cardiac sympathetic activity. In our laboratory, the normal value for the delayed H/M ratio is 2.1 to 2.7.

Statistical analysis

Continuous data are expressed as the mean ± SD. For comparisons between more than two groups, one-way analysis of variance and Dunn's multiple comparison test were used. Comparisons of continuous data between two patient groups were performed using the Mann-Whitney U test. Fisher's exact test was used to compare dichotomous data between two patient groups. All statistical tests were two-sided. A probability value of<.05 was considered significant.

Results

Dyssynchrony and Cardiac Sympathetic Activity in Non-ischemic HF and Pulmonary Hypertension

The results of the cross-correlation analysis of the circumferential strain

showed that of the 27 patients with non-ischemic HF, 12 had spatial dyssynchrony (44%) and 15 patients did not; 5 patients had temporal dyssynchrony (19%) and 22 did not. Out of the 16 patients with DCM, 7 had spatial dyssynchrony (44%) and 9 patients did not; 4 patients had temporal dyssynchrony (25%) and 12 did not. Out of the 5 patients with HT, 4 had spatial dyssynchrony (80%) and 1 patient did not; non-patient had temporal dyssynchrony (0%) and 5 did not. Out of the 9 patients with pulmonary hypertension, 2 had spatial dyssynchrony (22%) and 7 patients did not; 1 patient had temporal dyssynchrony (11%) and 8 did not.

The temporal dyssynchrony time was 80 ± 36 milliseconds for patients with non-ischemic HF and 72 ± 28 milliseconds for patients with pulmonary hypertension. The delayed H/M ratio was significantly lower for the 27 patients with non-ischemic HF compared to the 9 patients with pulmonary hypertension (2.0 ± 0.3 vs 2.5 ± 0.4, $P<.005$).

Relation Between Dyssynchrony and Cardiac Sympathetic Activity in Non-ischemic HF

The delayed H/M ratio was significantly lower for the 12 patients with spatial dyssynchrony compared to the 15 patients without (1.8 ± 0.3 vs 2.1 ± 0.3, P<.05). There was no significant difference in the delayed H/M ration between the patients with and without temporal dyssynchrony (2.0 ± 0.2 vs 2.0 ± 0.3) (Figure 3). The incidence of spatial dyssynchrony was significantly higher in the patients with a delayed H/M ratio <2.0 than those whose ratios were ≧2.0 [75% (9/12) vs 20% (3/15), P<.01]. There was no difference in the incidence of temporal dyssynchrony between patients with a delayed H/M ratio<2.0 and ≧2.0 [17% (2/12) vs 20% (3/15)] (Figure 4).

Relation Between Dyssynchrony and LV Function and Between Dyssynchrony and QRS Width in Non-ischemic HF

No significant difference in LVEF was observed between the patients with and without spatial dyssynchrony (26 ± 11% vs 29 ± 13%) or between the patients with and without temporal dyssynchrony (29 ± 19% vs 28 ± 11%) (Figure 5). No significant difference in QRS width was observed between the patients with and without spatial dyssynchrony (110 ± 28 vs 103 ± 18 milliseconds) or between the patients with and

without temporal dyssynchrony (103 ± 10 vs 107 ± 25 milliseconds).

Relation Between Cardiac Sympathetic Activity and BNP and Between Dyssynchrony and BNP in Non-ischemic HF

BNP was significantly greater for the patients with a delayed H/M ratio <2.0 than those whose ratios were ≧2.0 (525 ± 473 vs 262 ± 302 pg/mL, P<.05). No significant difference in BNP width was observed between the patients with and without spatial dyssynchrony (446 ± 473 vs 325 ± 342 pg/mL) or between the patients with and without temporal dyssynchrony (474 ± 408 vs 358 ± 407 pg/mL).

Patients Who Underwent CRT or LVAD

In 4 patients who underwent CRT, 1 patient had spatial dyssynchrony and 3 patients did not; 1 patient had temporal dyssynchrony and 3 patients did not. The mean delayed H/M ratio was 2.1.

In 2 patients who underwent LVAD, 1 patient had spatial dyssynchrony and 1 patient did not; 2 patients did not have temporal dyssynchrony. The mean delayed H/M

ratio was 1.8.

Discussion

In this study, the cross-correlation analysis of the myocardial strain time-curves using tagging MRI enabled the quantification of temporal dyssynchrony in patients with moderate to severe HF patients and also the qualitative assessment of spatial dyssynchrony. Our results demonstrated that cardiac sympathetic activity as assessed by MIBG scintigraphy was significantly less in HF patients with spatial dyssynchrony than in those without, even though the LVEF of the two groups was not significantly different. In contrast, there was no difference in the cardiac sympathetic activity between the patients with and without temporal dyssynchrony. These results suggest that cardiac sympathetic activity is related to the presence of LV dyssynchrony in patients with non-ischemic HF, and that spatial dyssynchrony causes a greater reduction in cardiac sympathetic activity compared to temporal dyssynchrony. The spatial dyssynchrony means the opposite systolic peaks on septal and lateral strain time curves. Visually, cine-MR imaging shows the dyskinetic wall motion in one of the two

segments and the paradoxical movement in the mainly septal wall. Manrique et al (18) reported that in DCM patients receiving modern medical therapy involving beta-blockers, I-123 MIBG uptake, but not intra-LV asynchrony, was predictive of clinical outcome. Their LV dyssynchrony was measured as the SD of the mean phase angle for the LV blood pools using ECG-gated myocardial perfusion scintigraphy. This nuclear phase analysis reflects the difference in contractile timing for each LV segments. Recently, Tanaka et al (19) measured temporal dyssynchrony by speckle-tracking echocardiography, and demonstrated the association between dyssynchrony and cardiac sympathetic activity assessed by MIBG uptake.

MRI has the potential to evaluate mechanical dyssynchrony either by tagging or velocity-encoded MRI. (20,21) Quantitative strain analysis based on circumferential myocardial activation data from tagging MRI has high spatial resolution, and has shown high reproducibility. Moreover, MRI data acquisition is largely operator and patient independent and may thus be better suited to characterize dyssynchronous HF and to identify appropriate candidates for CRT than Doppler echocardiographic methods. MRI myocardial tagging can be used to calculate local myocardial motion or strain.

Advances in the rapid analysis of tagged magnetic resonance images such as harmonic phase (HARP) (22) and the Sine-wave modeling approach, (23) and the design of novel global indexes of cardiac dyssynchrony may provide a more comprehensive method for selecting candidates for CRT. Tagged MRI is better able to assess spatial dyssynchrony than echocardiographic and radionuclide methods. Our proposing spatial dyssynchrony demonstrates the geometrical difference in LV contraction, and there appears to be some trade-off in our MRI approach of maximizing spatial resolution as opposed to maximizing temporal resolution. Spatial dyssynchrony may be an independent predictor of prognosis in HF from LV systolic function and BNP. On the other hand, temporal resolution of tagging MRI may be 30 to 50 milliseconds per frame, and is inferior to that of echocardiography. The assessment of spatial dyssynchrony compensates the limitation regarding temporal resolution, whereas the assessment of temporal dyssynchrony by tagging MRI may become rougher than that by echocardiography. This may lead the result that spatial dyssynchrony was more closely related to HF severity than temporal dyssynchrony. In 5 HF patients with temporal dyssynchrony, there were 4 with DCM and 1 with secondary cardiomyopathy. Their mean LV

end-diastolic volume was 259 mL and larger than the mean for all HF patients (189 mL). This suggests that temporal dyssynchrony may be related to physical dilated LV volume.

Jacobson et al (24) reported that among the commonly used LV functional parameters, an adrenergic neuronal functional parameter (H/M ratio) obtained by MIBG scan is an important and independent parameter for predicting sudden death in patients with HF. Autonomic dysfunction assessed by MIBG is thought to play an important role in the detection of high-risk ventricular arrhythmia. (25,26) Particularly, MIBG may identify the areas of denervation hypersensitivity, which cause ventricular arrhythmias. The areas of denervation hypersensitivity was found in myocardial scar and the around as assessed by myocardial perfusion imaging.(27) In ischemic and non-ischemic cardiomyopathy, akinesis and dyskinesis wall motion abnormalities were often seen in the myocardial scar including peri-scar areas.(28) With the progress of the myocardial fibrosis and scar in non-ischemic cardiomyopathy, a paradoxical wall movement in the mainly septal wall appears in the high frequency, corresponding to spatial dyssynchrony. The myocardial fibrosis relates to the tight in both sympathetic denervation

hypersensitivity and spatial dyssynchrony. This pathophysiological substrate can explain the lower delayed H/M ratios in patients with spatial dyssynchrony. (29)

CRT has been shown to reduce dyssynchrony and improve symptoms, quality of life, and exercise capacity in patients with HF. (30) Nevertheless, 30% to 40% of HF patients do not respond to CRT. (31,32) The H/M ratio and washout rate as assessed by MIBG were reported to be associated with the patient response to CRT, and the study's authors contended that the H/M ratio was an independent predictor of CRT response. (33) Higuchi et al (34) demonstrated that CRT can improve cardiac sympathetic activity as assessed by H/M ratio in patients with moderate to severe HF.

These findings support the detrimental effects of LV dyssynchrony on cardiac sympathetic activity. However, we were unable to determine the predictive value of the H/M ratio for the response to CRT because our study had only four patients who were treated with CRT. A particularly important parameter for the lack of response to CRT is the absence of mechanical dyssynchrony. This means that the identification of responders using time delay indexes alone is inherently limited. Thus, the assessment of LV dyssynchrony with the combination of spatial and temporal dyssynchrony and

delayed H/M ratio may enhance the ability to identify HF patients with a good chance of responding to CRT.

Limitations

This study examined a small number of patients at a single center. In general, a QRS width of 120 or 130 milliseconds is used as the definition of dyssynchrony. (35) The patients in this study had limited temporal dyssynchrony with a mean QRS duration of 102 milliseconds. The patient selection is biased against temporal dyssynchrony. Consequently, our study had fewer patients with the indication for CRT. The presence of dyssynchrony and delayed H/M ratio could not be examined as the indication for CRT or the predictor for CRT responder. Although the cut-off 110 milliseconds of temporal dyssynchrony was relative short, the temporal dyssynchrony time was 80 ± 36 milliseconds for 27 patients with non-ischemic HF and 72 ± 28 milliseconds for 9 patientswith pulmonary hypertension. The cut-off is thought adequate from the found value obtained from tagged MRI when their mean plus standard deviation was made a threshold.

The patients with pulmonary hypertension who had no LV dysfunction (mean LVEF 57%) were included as controls for LV failure. The cut-off of the delayed H/M ratio of 2.0 was higher than that shown to have prognostic significance in the ADMIRE-HF study. (24) As for one reason why the cut-off 2.0 was chosen, the mean and median delayed H/M ratio for patients with nonischemic HF was 2.0. Second, the mean minus standard deviation for patients with pulmonary hypertension was 2.1. The patients with pulmonary hypertension sometimes have interventricular septum shift toward LV cavity. This might cause two patients with spatial dyssynchrony in 9 patients with pulmonary hypertension. LVEF for the two patients were 71% and 54%. The pathophysiology of this septum abnormal wall motion is different from the LV dyssynchrony in HF, and does not influence LV function.

Conclusion

The cross-correlation analysis of the short-axis 2D tagging images enables the quantification of temporal and spatial dyssynchrony together. Cardiac sympathetic activity was found to be associated with the presence of LV dyssynchrony in patients

with non-ischemic HF. Spatial dyssynchrony demonstrates the geometrical difference in LV contraction, and is associated with a greater reduction in cardiac sympathetic activity.

References

1. Bohm M, La Rosee K, Schwinger RH, Erdmann E. Evidence for reduction of norepinephrine uptake sites in the failing human heart. J Am Coll Cardiol 1995;25:146-53.
2. Manger WM, Hoffman BB. Heart imaging in the diagnosis of pheochromocytoma and assessment of catecholamine uptake. J Nucl Med 1983;24:1194-6.
3. Glowniak JV, Turner FE, Gray LL, Palac RT, Lagunas-Solar MC, Woodward WR. Iodine-123 metaiodobenzylguanidine imaging of the heart in idiopathic congestive cardiomyopathy and cardiac transplants. J Nucl Med 1989;30:1182-91.
4. Merlet P, Pouillart F, Dubois-Rande JL, Delahaye N, Fumey R, Cataigne A, et al. Sympathetic nerve alterations assessed with 123IMIBG in the failing human heart. J Nucl Med 1999;40:224-31.
5. Schofer J, Spielmann R, Schuchert A, Weber K, Schluter M. Iodine-123 meta-iodobenzylguanidine scintigraphy: A noninvasive method to demonstrate myocardial adrenergic nervous system disintegrity in patients with idiopathic dilated cardiomyopathy. J Am Coll Cardiol 1988;12:1252-8.

6. Agostini D, Verberne HJ, Burchert W, Knuuti J, Povinec P, Sambuceti G, et al. I-123-mIBG myocardial imaging for assessment of risk for a major cardiac event in heart failure patients: Insights from a retrospective European multicenter study. Eur J Nucl Med Mol Imaging 2008;35:535-46.
7. Merlet P, Benvenuti C, Moyse D, Pouillart F, Dubois-Rande JL, Duval AM, et al. Prognostic value of MIBG imaging in idiopathic dilated cardiomyopathy. J Nucl Med 1999;40:917-23.
8. Nakata T, Miyamoto K, Doi A, Sasao H, Wakabayashi T, Kobayashi H, et al. Cardiac death prediction and impaired cardiac sympathetic innervation assessed by MIBG in patients with failing and nonfailing hearts. J Nucl Cardiol 1998;5:579-90.
9. Kalra PR, Sharma R, Shamim W, Doehner W, Wensel R, Bolger AP, et al. Clinical characteristics and survival of patients with chronic heart failure and prolonged QRS duration. Int J Cardiol 2002;86:225-31.
10. Gersh BJ, Maron BJ, Bonow RO, Dearani JA, Fifer MA, Link MS, et al. ACCF/AHA guideline for the diagnosis and treatment of hypertrophic cardiomyopathy: Executive summary: A report of the American College of

Cardiology Foundation/American Heart Association Task Force on Practice Guidelines. Circulation 2011;124:2761-96.

11. Manolio TA, Baughman KL, Rodeheffer R, Pearson TA, Bristow JD, Michels VV, et al. Prevalence and etiology of idiopathic dilated cardiomyopathy (summary of a National Heart, Lung, and Blood Institute workshop. Am J Cardiol 1992;69:1458-66.

12. Mestroni L, Maisch B, McKenna WJ, Schwartz K, Charron P, Rocco C, et al. Guidelines for the study of familial dilated cardiomyopathies. Collaborative Research Group of the European Human and Capital Mobility Project on Familial Dilated Cardiomyopathy. Eur Heart J 1999;20:93-102.

13. Okin PM, Devereux RB, Nieminen MS, Jerm S, Oikarinen L, Viltasaio M, et al. Electrocardiographic strain pattern and prediction of cardiovascular morbidity and mortality in hypertensive patients. Hypertension 2004;44:48-54.

14. Topol EJ, Traill TA, Fortuin NJ. Hypertensive hypertrophic cardiomyopathy of the elderly. N Engl J Med 1985;312:277-83.

15. Galie N, Hoeper MM, Humbert M, Torbicki A, Vachiery JL, Barbera JA, et al. Guidelines for the diagnosis and treatment of pulmonary hypertension. Eur Respir J 2009;34:1219-63.

16. Arts T, Prinzen FW, Delhaas T, Milles JR, Rossi AC, Clarysse P. Mapping displacement and deformation of the heart with local sine-wave modeling. IEEE Trans Med Imaging 2010;29:1114-23.

17. Fornwalt BK, Arita T, Bhasin M, Voulgaris G, Merlino JD, Leon AR, et al. Cross-correlation quantification of dyssynchrony: A new method for quantifying the synchrony of contraction and relaxation in the heart. J Am Soc Echocardiogr 2007;20:1330 e1-1337 e1.

18. Manrique A, Bernard M, Hitzel A, Bauer F, Menard JF, Sabatier R, et al. Prognostic value of sympathetic innervation and cardiac asynchrony in dilated cardiomyopathy. Eur J Nucl Med Mol Imaging 2008;35:2074-81.

19. Tanaka H, Tatsumi K, Fujiwara S, Tsuji T, Kaneko A, Ryo K, et al. Effect of left ventricular dyssynchrony on cardiac sympathetic activity in heart failure patients with wide QRS duration. Circ J 2012;76:382-9.

20. Lardo AC, Abraham TP, Kass DA. Magnetic resonance imaging assessment of ventricular dyssynchrony: Current and emerging concepts. J Am Coll Cardiol 2005;46:2223-8.

21. Epstein FH. MRI of left ventricular function. J Nucl Cardiol 2007;14:729-44.

22. Osman NF, Prince JL. Visualizing myocardial function using HARP MRI. Phys Med Biol 2000;45:1665-82.

23. Nagao M, Hatakenaka M, Matsuo Y, Kamitani T, Higuchi K, Shikata F, et al. Subnedocardial contractile impairment in chronic ischemic myocardium: Assessment by strain analysis of 3T tagged CMR. J Cardiovasc Magn Reson 2012;14:14.

24. Jacobson AF, Senior R, Cerqueira MD, Wong ND, Thomas GS, Lopez VA, et al. Myocardial iodine-123 meta-iodobenzylguanidine imaging and cardiac events in heart failure. Results of the prospective ADMIRE-HF (AdreView Myocardial Imaging for Risk Evaluation in Heart Failure) study. J Am Coll Cardiol 2010;55:2212-21.

25. Podrid PJ, Fuchs T, Candinas R. Role of the sympathetic nervous system in the

genesis of ventricular arrhythmia. Circulation 1990;82:I103-13.

26. Zipes DP. Sympathetic stimulation and arrhythmias. N Engl J Med 1991;325:656-7.

27. Nishisato K, Hashimoto A, Nakata T, Doi T, Yamamoto H, Nagahara D, et al. Impaired cardiac sympathetic innervation and myocardial perfusion are related to lethal arrhythmia: Quantification of cardiac tracers in patients with ICDs. J Nucl Med 2010;51:1241-9.

28. Inoue Y, Yang X, Nagao M, Higashino H, Hosokawa K, Kido T, et al. Peri-infarct dysfunction in post-myocardial infarction: Assessment of 3-T tagged and late enhancement MRI. Eur Radiol 2010;20:1139-48.

29. Adelstein EC, Tanaka H, Soman P, Miske G, Haberman SC, Sabe SF, et al. Impact of scar burden by single-photon emission computed tomography myocardial perfusion imaging on patient outcomes following cardiac resynchronization therapy. Eur Heart J 2011;32:93-103.

30. Stahlberg M, Braunschweig F, Gadler F, Karlsson H, Linde C. Three year outcome of cardiac resynchronization therapy: A single center evaluation. Pacing Clin Electrophysiol 2005;28:1013-7.

31. Abraham WT, Fisher WG, Smith AL, Delurgio DB, Leon AR, Loh E, et al. Cardiac resynchronization in chronic heart failure. N Engl J Med 2002;346:1845-53.

32. Bax JJ, Bleeker GB, Marwick TH, Molhoek SG, Boersma E, Steendijk P, et al. Left ventricular dyssynchrony predicts response and prognosis after cardiac resynchronization therapy. J Am Coll Cardiol 2004;44:1834-40.

33. Nishioka SA, Martinelli Filho M, Brandao SC, Giorgi MC, Vieira ML, et al. Cardiac sympathetic activity pre and post resynchronization therapy evaluated by 123I-MIBG myocardial scintigraphy. J Nucl Cardiol 2007;14:852-9.

34. Higuchi K, Toyama T, Tada H, Naito S, Ohshima S, Kurabayashi M. Usefulness of biventricular pacing to improve cardiac symptoms, exercise capacity and sympathetic nerve activity in patients with moderate to severe chronic heart failure. Circ J 2006;70:703-9.

35. Pitzalis MV, Iacoviello M, Romito R, Massari F, Rizzon B, Luzzi G, et al. Cardiac resynchronization therapy tailored by echocardiographic evaluation of ventricular asynchrony. J Am Coll Cardiol 2002;40:1615-22.

Table 1. Characteristics of the heart failure patinents

	All patients	DCM	pH	HT	Others
Clinical characteristics					
No. of patients (%)	36	16 (44)	9 (25)	5 (14)	6 (17)
Males (%)	21 (58)	12 (75)	2 (22)	3 (60)	4 (67)
Age (mean ± SD)	47 ± 17	43 ± 18	50 ± 16	56 ± 8	46 ± 20
Diabetes (%)	7 (19)	4 (25)	0 (0)	3 (60)	0 (0)
Hypertension (%)	10 (28)	3 (19)	1 (11)	5 (100)	1 (17)
Hypercholesterolemia (%)	6 (17)	2 (13)	0 (0)	3 (60)	1 (17)
Current smoker (%)	14 (39)	9 (56)	0 (0)	3 (60)	2 (33)
QRS duration (mean ± SD)	102 ± 22	104 ± 15	89 ± 10	94 ± 5	122 ± 40
CLBBB (%)	1 (3)	1 (6)	0 (0)	0 (0)	0 (0)
Systolic blood pressure (mm Hg)	99 ± 21	94 ± 13	116 ± 14	101 ± 27	86 ± 30
Diastolic blood pressure (mm Hg) (mean ± SD)	61 ± 12	57 ± 11	66 ± 8	59 ± 16	64 ± 14
Heart rate (bpm) (mean ± SD)	77 ± 11	77 ± 14	79 ± 8	74 ± 10	75 ± 10
New York Heart Association mean					
Class II	14 (39)	6 (38)	3 (33)	1 (20)	4 (67)
Class III	19 (53)	7 (44)	6 (67)	4 (80)	2 (33)
Class IV	3 (8)	3 (19)	0 (0)	0 (0)	0 (0)
CMR characteristics (mean ± SD)					
LVEDV (mL)	189 ± 110	242 ± 132	105 ± 20	222 ± 69	145 ± 55
LVESV (mL)	136 ± 103	193 ± 115	45 ± 9	168 ± 71	94 ± 47
Ejection fraction (%)	35 ± 18	26 ± 16	57 ± 8	26 ± 12	38 ± 12
LV mass (g)	135 ± 54	153 ± 63	103 ± 30	181 ± 46	109 ± 7
LVEDV index (mL/m^2)	115 ± 61	147 ± 73	71 ± 14	123 ± 27	92 ± 41
LVESV index (mL/m^2)	82 ± 58	116 ± 64	31 ± 6	93 ± 32	60 ± 35
LV mass index (g/m^2)	84 ± 30	93 ± 36	70 ± 22	102 ± 24	69 ± 1

CLBBB, Complete left bundle block; *LVEDV*, left ventricular end-diastole volume; *LVESV*, left ventricular end-systole volume

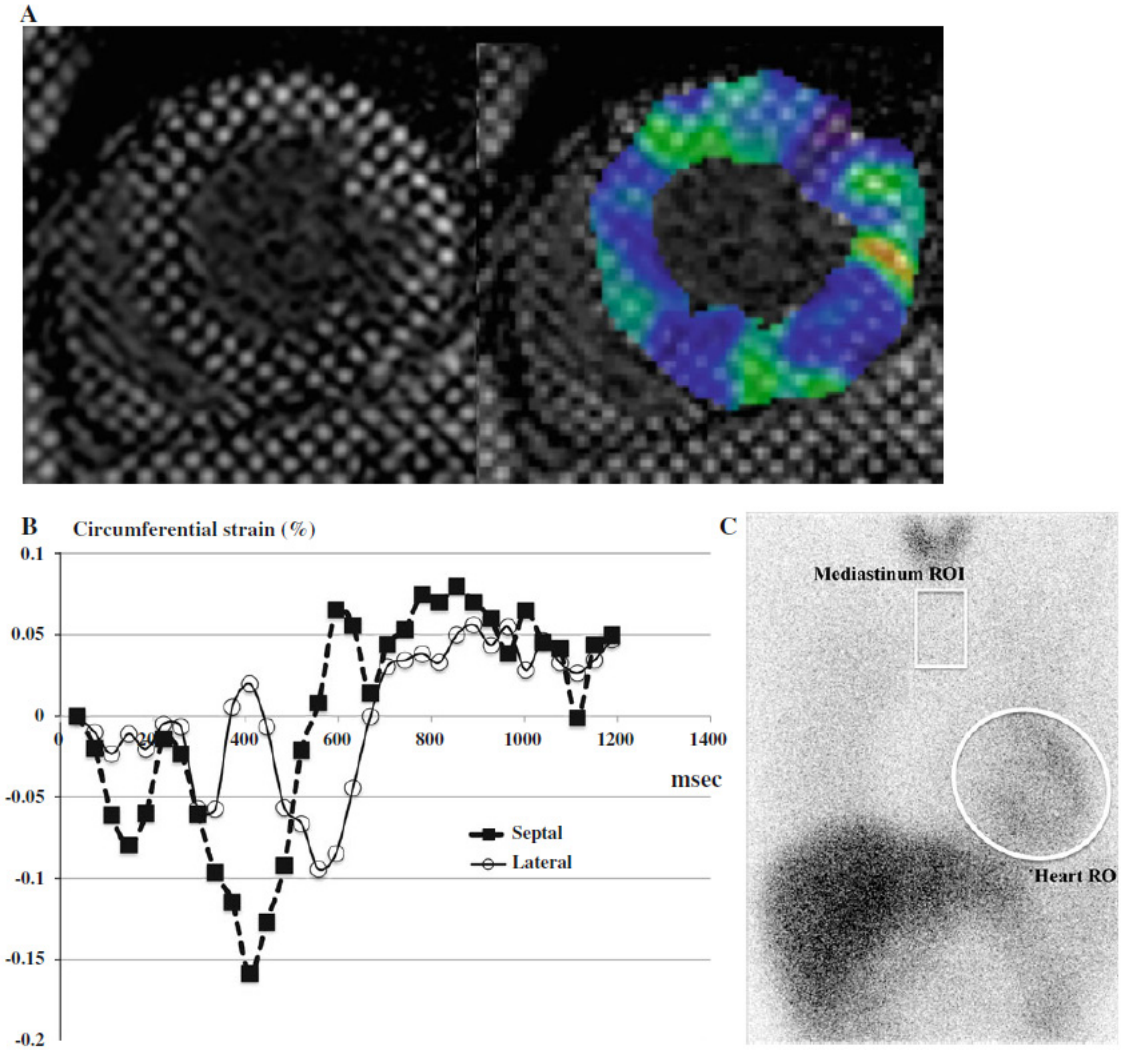

Figure. 1. An 18-year-old man with DCM. A Short-axis mid-ventricular views of cine-tagging MR images at end-systole (left). The inTag Osirix software for tag analysis automatically plotted the area of the left ventricle and produced a color-coded strain map that shows low values as cold colors and high value as hot colors (right). B Circumferential strain time curves for mid-septal and midlateral segments. The x-axis indicates time (milliseconds) and the y-axis indicates the circumferential value. The

time to reach a negative peak value from the time curve of the mid-lateral segment is late for the mid-septal segment. The cross-correlation delay time is 111 milliseconds. C Calculation of metaiodobenzylguandine (MIBG) heart-to-mediastinum (H/M)ratio based on an anterior view of the thorax at delayed scan. Regions of interest (ROIs) have been drawn over the heart and mediastinum. His delayed H/M ratio is 2.1.

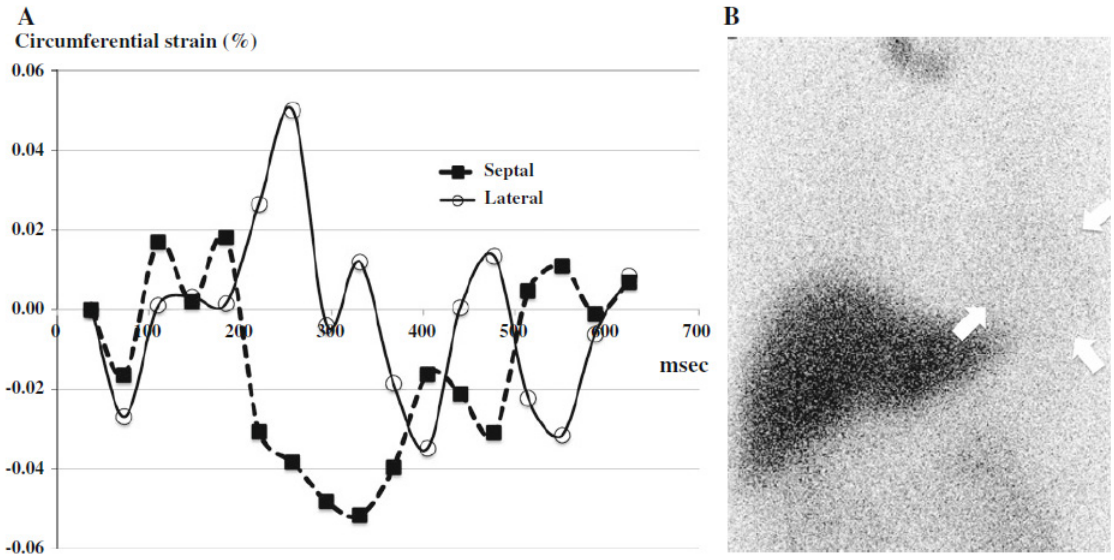

Figure. 2. A 62-year-old man with DCM. A Circumferential strain time curves for mid-septal and mid-lateral segments. The x-axis indicates time (milliseconds) and the y-axis indicates the circumferential value. The strain time curves for the septal segment has a downward curve and a negative peak during mid- to end-systole, whereas that for

the lateral segment has an upward curve and a positive peak at early to mid-systole. The systolic peaks for the two time curves are opposite, which indicates the spatial dyssynchrony. The cross-correlation delay time is 111 milliseconds. B The anterior view of the thorax on delayed MIBG imaging shows faint accumulation in the left ventricle (arrows). His delayed H/M ratio is 1.4.

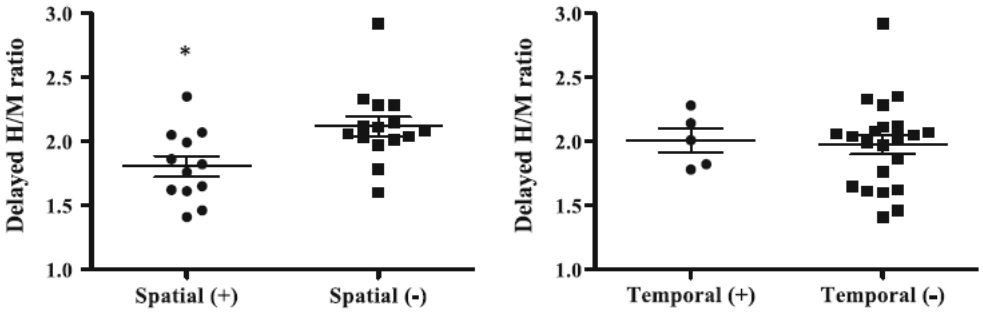

Figure. 3. Scatterplot showing the delayed H/M ratio for the patients with and without spatial dyssynchrony (left) and temporal dyssynchrony (right). Horizontal long line Mean value of the delayed H/M ratios; upper and lower short lines standard error of the mean. The delayed H/M ratio was significantly lower for the 12 patients with spatial dyssynchrony compared to the 15 patients without. There was no significant difference between the patients with and without temporal dyssynchrony. *P<.05.

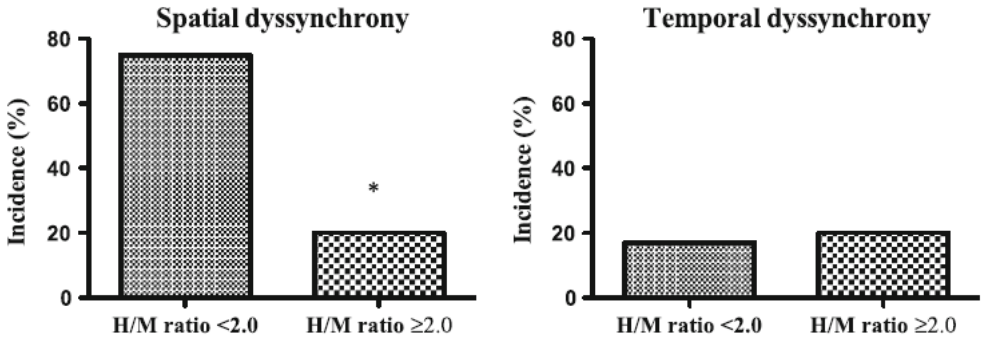

Figure. 4. Incidence of spatial dyssynchrony (left) and temporal dyssynchrony (right) by the delayed H/M ratio. The incidence of spatial dyssynchrony was significantly higher in the patients with a delayed H/M ratio<2.0 than those whose ratios were≧2.0. There was no difference in the incidence of temporal dyssynchrony between patients with a delayed H/M ratio<2.0 and ≧2.0.

*P<.01.

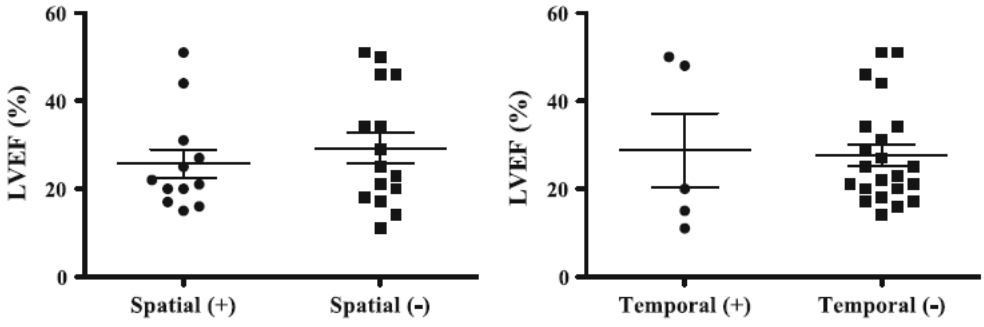

Figure. 5. Scatterplot showing LVEF for the patients with and without spatial

dyssynchrony (left) and temporal dyssynchrony (right). Horizontal long line Mean value of the LVEF; upper and lower short lines standard error of the mean. There was no significant difference in LVEF between the patients with and without dyssynchrony of both types.